

## Synthesis of Millimeter-Range Orthorhombic $V_2O_5$ Nanowires and Impact of Thermodynamic and Kinetic Properties of the Oxidant on the Synthetic Process

Fu Zhou,<sup>\*,[a]</sup> Xuemei Zhao,<sup>[a]</sup> Yunqi Liu,<sup>[a]</sup> Cunguang Yuan,<sup>[a]</sup> and Li Li<sup>[a]</sup>

**Keywords:** Nanostructures / Crystal growth / Layered compounds

Large-scale orthorhombic  $V_2O_5$  single-crystalline nanowires with diameters of 60–80 nm and lengths into the millimeter range were synthesized through a facile template-free, mild, and direct hydrothermal reaction between  $VOSO_4 \cdot xH_2O$  and  $KMnO_4$ . The nanowires are nearly visible to the naked eye and are by far the longest 1D nanostructures of vanadium oxide ever fabricated. The impacts of the thermodynamic

and kinetic properties of the oxidant were studied by parallel experiments by using different kinds of oxidants, and both were found to be crucial for the successful synthesis of the ultralong  $V_2O_5$  nanowires.

(© Wiley-VCH Verlag GmbH & Co. KGaA, 69451 Weinheim, Germany, 2008)

### Introduction

Vanadium oxide and derived compounds have received significant attention recently because of their structural versatility combined with their unique chemical and physical properties.<sup>[1]</sup> Like most transitional metals, vanadium can exist in different valence states and consequently form a variety of binary vanadium oxides with the general formula  $VO_{2+x}$  ( $0 \leq x \leq 0.33$ ), such as  $V_2O_5$ ,  $V_2O_3$ ,  $V_6O_{13}$ ,  $VO_2$ , and so on. These compounds have attracted great attention because of their outstanding properties and potential applications as catalysts, chemistry sensors, high-energy density lithium-ion batteries, and electrochemical and optical devices.<sup>[2–4]</sup>

In the last decade, great attention has been focused on the synthesis and applications of nanostructured materials, and one of the most dynamic research areas is one-dimensional (1D) nanostructures, such as nanowires, nanorods, nanobelts, and nanotubes.<sup>[5–8]</sup> Recently, the fabrication of vanadium oxide 1D nanostructures has been researched intensively. A variety of methods, such as thermal evaporation, surfactant-assisted solution, and hydrothermal/solvothermal synthesis, have been developed to prepare vanadium oxide 1D nanostructures.<sup>[9–12]</sup> Cao et al. have made many efforts on the synthesis of  $V_2O_5$  1D nanostructures and their subsequent application in the electrochemical field.<sup>[13–17]</sup> The group of Ha has done a lot of research on the synthesis and properties of  $V_2O_5$  nanowires.<sup>[18,19]</sup> Martin et al. have made great contributions in the possible applications of  $V_2O_5$  1D nanostructures in the lithium-ion

battery industry.<sup>[20–22]</sup> However, all these synthetic methods of vanadium oxide 1D nanostructures are either based on the transformation of  $V^{5+}$ -contained precursors during reaction or through a complex and lengthy route. To the best of our knowledge, the simple direct hydrothermal synthesis of  $V_2O_5$  1D nanostructures from reagents in which vanadium possesses a +4 oxidation state has been rarely reported. Recently, our group published a paper on the successful hydrothermal synthesis of orthorhombic  $V_2O_5$  nanowires by oxidation of  $VOSO_4 \cdot xH_2O$  by  $KMnO_4$ .<sup>[23]</sup> However, there is currently no established criteria for the choice of oxidants for the successful synthesis of  $V_2O_5$  nanowires.

In this communication, we report the study on the criteria for the selection of oxidants for the fabrication of  $V_2O_5$  nanowires by using  $V^{IV}$  reagents as precursors. Our research results indicate that both the thermodynamic properties of the oxidant, which determine the oxidizing ability of the oxidizer, and the kinetic properties of the oxidant, which determine the velocity of the oxidation reaction, are decisive factors contributing to the phase and morphology of the final products. The criteria for the choice of oxidants are established on the basis of our research.

### Results and Discussion

For the fabrication of orthorhombic  $V_2O_5$  nanowires, all the reagents were of analytical grade and were used without further purification. In a typical synthetic procedure of orthorhombic  $V_2O_5$  nanowires,  $VOSO_4 \cdot xH_2O$  (10 mmol) and  $KMnO_4$  (5 mmol) were dissolved in distilled water (40 mL), and the mixture was stirred magnetically for 30 min to obtain homogeneity. Nitric acid was added dropwise whilst

[a] Department of Chemistry, China University of Petroleum, Qingdao, Shandong 266555, P. R. China  
Fax: +86-532-86981318  
E-mail: boksiczf@ustc.edu

stirring until the final pH of the solution was about 1–2. The resulting clear solution was then transferred into a 50-mL Teflon-lined stainless-steel autoclave. The autoclave was maintained at 160 °C for 24 h. After cooling to room temperature naturally, the yellow silk-like precipitates were filtered off, washed several times with distilled water and anhydrous alcohol, and dried in vacuo at 80 °C for 12 h. For comparative experiments, only KClO<sub>3</sub> or K<sub>2</sub>S<sub>2</sub>O<sub>8</sub> was used instead of KMnO<sub>4</sub> as the oxidant, and all other synthesis parameters and reaction process were the same as before.

XRD patterns of the final products were recorded by using a Philips X'Pert Super diffractometer with graphite monochromated Cu-*K*<sub>α</sub> radiation ( $\lambda = 1.54178 \text{ \AA}$ ) in the  $2\theta$  range of 5–80°. Figure 1 shows the XRD pattern of the typical product with the use of KMnO<sub>4</sub> as the oxidant. All the diffraction peaks could be indexed as the orthorhombic phase of V<sub>2</sub>O<sub>5</sub> and are in agreement with literature values (JCPDS card 85-0601); calculated lattice constants are  $a = 3.563 \text{ \AA}$ ,  $b = 11.516 \text{ \AA}$ ,  $c = 4.374 \text{ \AA}$ . The (001) peak was extraordinarily strong relative to other peaks, which differed greatly from the XRD data for the powder sample (JCPDS card 85-0601); this indicates that the as-obtained orthorhombic V<sub>2</sub>O<sub>5</sub> might have special morphologies. To further testify if residual manganese remained in the final product, it was subjected to an AA (atomic absorption) test, which proved that the manganese content in the final product was nearly zero. On the basis of the results of XRD and the AA test, it is clear that pure orthorhombic phase of V<sub>2</sub>O<sub>5</sub> was successfully prepared by our synthetic route.

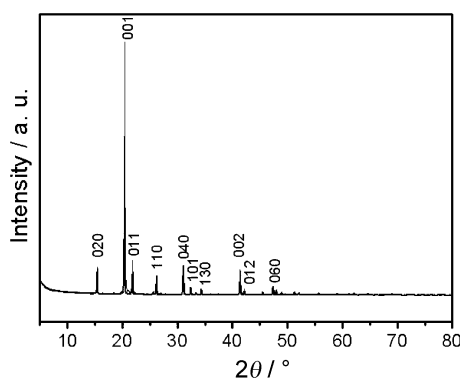


Figure 1. XRD pattern of the typical product by using KMnO<sub>4</sub> as the oxidant.

Figure 2 a,b show the field emission scanning electron microscopy (FESEM, JEOL JSM – 6300F, 15 kV) images of the typical product with KMnO<sub>4</sub> as the oxidant. The microstructures of the product were long uniform nanowires, and the proportion of the nanowires in the sample was almost 100% (Figure 2 b). The length of the as-obtained orthorhombic V<sub>2</sub>O<sub>5</sub> nanowires reached nearly 1 mm, as calculated from the panoramic image shown in Figure 2a. The nanowires are almost visible to the naked eye, and they are by far the longest 1D vanadium oxide nanostructures fabricated to date, which indicates the high efficiency of our synthetic method. The diameters of the

nanowires ranged from 60 to 80 nm (Figure 2b), and the as-obtained nanowires had a strong tendency to self-assemble into nanowire arrays. TEM images (Hitachi 800 TEM, 200 kV) of the typical product with KMnO<sub>4</sub> as the oxidant are given in Figure 2c,d, which clearly shows that nanowire arrays of orthorhombic V<sub>2</sub>O<sub>5</sub> with diameters around 60 nm and lengths up into the millimeter range were obtained. The inset SAED image in Figure 2d provides evidence that the as-obtained V<sub>2</sub>O<sub>5</sub> nanowires are singly crystalline.

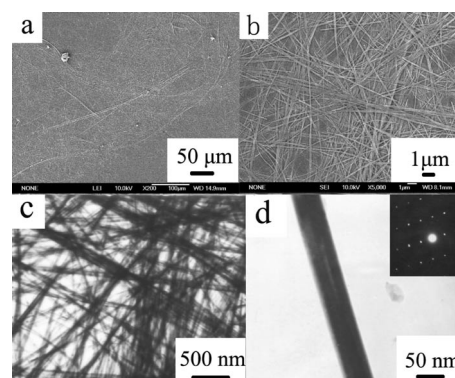


Figure 2. FESEM (a and b) and TEM (c and d) images of the typical product by using KMnO<sub>4</sub> as the oxidant.

The morphologies and microstructures of the nanowires were also characterized by using high-resolution transmission electron microscopy (HRTEM; JEOL-2010) with an acceleration voltage of 200 kV. The HRTEM image of a typical orthorhombic V<sub>2</sub>O<sub>5</sub> nanowire is shown in Figure 3a,b. The distance between the neighboring planes is about 0.287 nm (Figure 3b), which is consistent with that of the (040) plane of orthorhombic V<sub>2</sub>O<sub>5</sub>; this is indicative of an individual nanowire growth direction of [010]. The inset SAED pattern in Figure 3a, taken from an individual nanowire, reveals its good single-crystal nature.

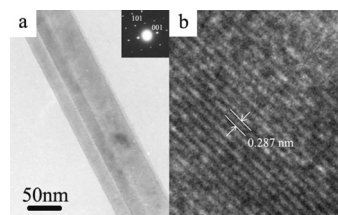


Figure 3. HRTEM images of the typical product by using KMnO<sub>4</sub> as the oxidant.

As no surfactant or any kind of template is used in our synthetic route, the only reason for the initial reagents to transform into the final ultralong nanowires is the oxidant. Thus, it would be an interesting topic to study the impact of the choice of different oxidants on the structure of the final product. We wanted to learn if there were any prerequisites for the oxidants to effectively produce the ultralong nanowires.

In order to make the qualification of the oxidant clear, two other different kinds of oxidants were chosen: K<sub>2</sub>S<sub>2</sub>O<sub>8</sub> and KClO<sub>3</sub>. The oxidation–reduction potentials ( $E^\circ$ ) in

acidic solution of the  $\text{S}_2\text{O}_8^{2-}/\text{SO}_4^{2-}$ ,  $\text{MnO}_4^-/\text{Mn}^{2+}$ , and  $\text{ClO}_3^-/\text{Cl}^-$  redox couples are 2.01, 1.51, and 1.45 V, respectively.<sup>[24]</sup> The XRD patterns of the as-obtained products by using  $\text{KClO}_3$  or  $\text{K}_2\text{S}_2\text{O}_8$  as the oxidant are shown in Figure 4a,b. All the diffraction can be ascribed to layered-phase  $\text{V}_2\text{O}_5 \cdot x\text{H}_2\text{O}$  with a large amount of  $\text{H}_2\text{O}$  molecules intercalated between the layers, which has been reported by other chemists.<sup>[25,26]</sup> It is clearly observed that by using these two oxidants, no orthorhombic  $\text{V}_2\text{O}_5$  phase can be obtained, which indicates that there must existed some qualifications for the oxidant to produce the orthorhombic  $\text{V}_2\text{O}_5$  phase.

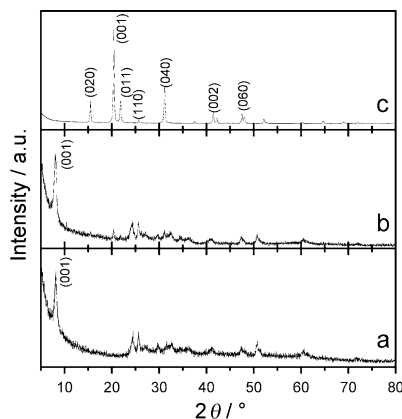


Figure 4. XRD patterns of the products by using (a)  $\text{KClO}_3$ , (b)  $\text{K}_2\text{S}_2\text{O}_8$ , (c)  $\text{K}_2\text{S}_2\text{O}_8$  and  $\text{AgNO}_3$  as the oxidants.

By analyzing the XRD patterns of the final product with  $\text{KClO}_3$  or  $\text{K}_2\text{S}_2\text{O}_8$  as the oxidant, the product is determined to be water intercalated layered phase  $\text{V}_2\text{O}_5 \cdot x\text{H}_2\text{O}$ .  $\text{K}_2\text{S}_2\text{O}_8$  and  $\text{KClO}_3$  do not expel the intercalated water out of the interlayer space of  $\text{V}_2\text{O}_5$  as effectively as  $\text{KMnO}_4$ . For  $\text{KClO}_3$ , it is rather easy to explain the phenomenon. Because the value of  $E^\circ$  for  $\text{ClO}_3^-/\text{Cl}^-$  is only 1.45 V, its oxidizing ability is too weak to drive the intercalated water out of the lattice. On the basis of this observation, it is odd that  $\text{KMnO}_4$  can effectively do this, as the value of  $E^\circ$  for  $\text{MnO}_4^-/\text{Mn}^{2+}$  is just 1.51 V, which is just a little higher than that of  $\text{ClO}_3^-/\text{Cl}^-$  (1.45 V). However, it should be noted that the value of  $E^\circ$  for  $\text{MnO}_4^-/\text{MnO}_2$  in an acidic environment is 1.70 V; thus, the necessary driving force for the removal of the  $\text{H}_2\text{O}$  molecules from the interplanar regions of the layered structures of  $\text{V}_2\text{O}_5 \cdot x\text{H}_2\text{O}$  can be supplied to obtain the orthorhombic  $\text{V}_2\text{O}_5$  phase. With the use of  $\text{KMnO}_4$  as the oxidant, it is believed that during the reaction process  $\text{MnO}_4^-$  is first reduced to  $\text{MnO}_2$  and then to  $\text{Mn}^{2+}$  as the final reduction product. However, the question as to why a strong oxidant such as  $\text{K}_2\text{S}_2\text{O}_8$ , which is a thermodynamically favorable reagent as an oxidizer [ $E^\circ(\text{S}_2\text{O}_8^{2-}/\text{SO}_4^{2-}) = 2.01$  V], was unable to drive out the intercalated water in the interlayer area of the  $\text{V}_2\text{O}_5 \cdot x\text{H}_2\text{O}$  phase is still not answered. This can be rationalized by the fact that the thermodynamic properties of the oxidant are not the only determining factor in the redox process: the kinetic character of the oxidant is also a decisive factor in this process. Reactions involving  $\text{K}_2\text{S}_2\text{O}_8$  as an oxidant tend to be rather

slow, even though  $\text{K}_2\text{S}_2\text{O}_8$  is a very strong oxidizer. A simple solution to this problem involves the use of cations as a catalyst, and one excellent choice is  $\text{Ag}^+$ . A parallel experiment was performed by using  $\text{K}_2\text{S}_2\text{O}_8$  as the oxidant and by keeping the reaction temperature and pH value unchanged; the only difference was the addition of  $\text{AgNO}_3$  ( $1 \text{ mol L}^{-1}$ , 1 mL) into the system, which served as a catalyst during the reaction process. Ultralong orthorhombic  $\text{V}_2\text{O}_5$  nanowires were successfully fabricated this time, which was proven by the XRD pattern (Figure 4c). The FESEM images were also very similar to those of the typical products by using  $\text{KMnO}_4$  as the oxidant and are thus not shown here.

## Conclusions

An environmentally friendly, template-free, and inexpensive synthesis method was developed for the fabrication of uniform orthorhombic  $\text{V}_2\text{O}_5$  nanowires with lengths up into the millimeter range. Thermodynamic and kinetic properties were shown to have an impact on the phase and morphology of the final products, which indicates that both are decisive factors in the successful production of  $\text{V}_2\text{O}_5$  nanowires. On the basis of our research, we believe that the oxidation–reduction potential of the oxidant should be greater than 1.5 V and that the velocity of the oxidation reaction should exceed a critical level. Further work is under way in our laboratory to study the electrochemical properties of these ultralong orthorhombic  $\text{V}_2\text{O}_5$  nanowires, and the results will be reported later.

- [1] P. Y. Zavalij, M. S. Whittingham, *Acta Crystallogr., Sect. B* **1999**, 55, 627–663.
- [2] N. Magg, J. B. Giorgi, M. M. Frank, B. Immaraporn, T. Schroeder, M. Baumer, H. J. Freund, *J. Am. Chem. Soc.* **2004**, 126, 3616–3626.
- [3] P. Liu, S. H. Lee, H. M. Cheong, C. E. Tracy, J. R. Pitts, R. D. Smith, *J. Electrochem. Soc.* **2002**, 149, 76–80.
- [4] G. Sudant, E. Baudrin, B. Dunn, J. M. Tarascon, *J. Electrochem. Soc.* **2004**, 151, A666–A671.
- [5] F. Zhou, H. G. Zheng, X. M. Zhao, Q. X. Guo, X. M. Ni, T. Shen, C. M. Tang, *Nanotechnology* **2005**, 16, 2072–2076.
- [6] F. Zhou, X. M. Zhao, H. Xu, C. G. Yuan, *Chem. Lett.* **2006**, 35, 1280–1281.
- [7] X. Wang, Y. D. Li, *Chem. Eur. J.* **2003**, 9, 300–306.
- [8] Z. W. Pan, Z. R. Dai, Z. L. Wang, *Science* **2001**, 291, 1947–1949.
- [9] P. M. Ajayan, O. Stepphan, P. Redlich, C. Colliex, *Nature* **1995**, 375, 564–567.
- [10] X. Chen, X. M. Sun, Y. D. Li, *Inorg. Chem.* **2002**, 41, 4524–4530.
- [11] S. Myung, M. Lee, G. T. Kim, J. S. Ha, S. H. Hong, *Adv. Mater.* **2005**, 17, 2361–2364.
- [12] S. J. Park, J. S. Ha, Y. J. Chang, G. T. Kim, *Chem. Phys. Lett.* **2004**, 390, 199–202.
- [13] K. Takahashi, Y. Wang, G. Z. Cao, *J. Phys. Chem. B* **2005**, 109, 48–51.
- [14] K. Takahashi, S. J. Limmer, Y. Wang, G. Z. Cao, *J. Phys. Chem. B* **2004**, 108, 9795–9800.
- [15] Y. Wang, K. Takahashi, H. M. Shang, G. Z. Cao, *J. Phys. Chem. B* **2005**, 109, 3085–3088.
- [16] Y. Wang, G. Z. Cao, *Chem. Mater.* **2006**, 18, 2787–2804.

- [17] G. Z. Cao, *J. Phys. Chem. B* **2004**, *108*, 19921–19931.
- [18] Y. K. Kim, S. J. Park, J. P. Koo, G. T. Kim, S. Hong, J. S. Ha, *Nanotechnology* **2007**, *18*, 015304.
- [19] J. P. Koo, Y. Kim, J. S. Ha, *Appl. Surf. Sci.* **2006**, *253*, 1528–1533.
- [20] B. B. Lakshmi, C. J. Patrissi, C. R. Martin, *Chem. Mater.* **1997**, *9*, 2544–2550.
- [21] C. J. Patrissi, C. R. Martin, *J. Electrochem. Soc.* **1999**, *146*, 3176–3180.
- [22] C. R. Slides, C. R. Martin, *Adv. Mater.* **2005**, *17*, 125–128.
- [23] F. Zhou, X. M. Zhao, C. G. Yuan, H. Xu, *Chem. Lett.* **2007**, *36*, 310–311.
- [24] *Lange's Handbook of Chemistry*, 13th ed., McGraw-Hill, New York, **1985**, chapter 8, table 8.27.
- [25] T. Yao, Y. Oka, N. Yamamoto, *Mater. Res. Bull.* **1992**, *27*, 669–675.
- [26] Y. Wang, H. M. Shang, T. Chou, G. Z. Cao, *J. Phys. Chem. B* **2005**, *109*, 11361–11366.

Received: February 8, 2008  
Published Online: April 24, 2008